Comparison of Radar Receivers for OFDM and OTFS waveforms

Correas-Serrano, Aitor; Petrov, Nikita; Gonzalez-Huici, Maria; Yarovoy, Alexander

DOI
10.23919/EuRAD54643.2022.9924824

Publication date
2022

Document Version
Final published version

Published in
2022 19th European Radar Conference, EuRAD 2022

Comparison of Radar Receivers for OFDM and OTFS waveforms

Aitor Correas-Serrano[#1], Nikita Petrov[*&2], Maria Gonzalez-Huici[#3], Alexander Yarovoy[&4]
[#]Fraunhofer FHR, Germany
[*]NXP Semiconductors, Netherlands
[&]TU Delft, Netherlands
{[1]Aitor.Correas, [3]Maria.Gonzalez}@fhr.fraunhofer.de, {[2]N.Petrov, [4]A.Yarovoy}@tudelft.nl

***Abstract* — A generic description for common multi-carrier radar receivers is proposed. Two multi-carrier waveforms - orthogonal frequency division multiplexing (OFDM) and orthogonal time-frequency spacing (OTFS) - which could be used for joint radar and communication (JRC) applications - are considered. Sensing performances of different waveform-receiver pairs are compared theoretically. It is shown that while qualitatively, both waveforms perform similarly under the same receiver, performance differences exist between them.**

***Keywords* — Orthogonal time-frequency spacing, Orthogonal frequency division multiplexing, multicarrier radar, integrated side lobe ratio, inter-carrier interference.**

I. Introduction

The advent of compact software-defined radar systems able to generate fully digital waveforms, together with the issue of the congested spectrum, has motivated research in systems able to perform both communication and sensing tasks in the same frequency bands. In this context, multicarrier waveforms based on orthogonal frequency division multiplexing (OFDM) are promising in achieving good radar and communications performance without significant changes in existing communication system design. OFDM suffers from inter-carrier interference (ICI) when subject to Doppler shifts above a tenth of the subcarrier separation due to the de-orthogonalization of the subcarriers, affecting both communications and radar performance [1]. Considering that the deployment of radar is often tied with high-mobility scenarios, ICI limits the implementation scenarios of OFDM joint radar and communication systems.

Recently, orthogonal time-frequency space (OTFS) modulation has gathered attention as an OFDM alternative for communications and radar in high-mobility scenarios. OTFS is a recent modulation proposed as an improvement over OFDM regarding Doppler tolerance. Similar to OFDM, OTFS uses the entire time-frequency plane to transmit information. Unlike OFDM, in which the symbols are defined over the frequency grid, OTFS symbols are defined over the "delay-Doppler" plane and spread over the time-frequency plane through the discrete symplectic Fourier transform (DSFT). Higher Doppler tolerance and a shorter cyclic prefix [2] make this waveform a potential improvement over OFDM modulations for radar and JRC.

The performance of OTFS and OFDM radar has been compared recently in both[3] and [4]. The authors of [3] derivate a maximum likelihood receiver for the OTFS waveform considering inter-symbol interference (ISI) and ICI and compare it with the symbol-canceling maximum likelihood receiver for an OFDM signal, which implicitly assumes no ISI/ICI. In [4], a more straightforward matched filter OTFS receiver is developed and compared with an unspecified OFDM radar receiver under moderate ICI conditions, showing a systematic Doppler estimation error in the latter. This effect is inconsistent with the previously reported effect of ICI in OFDM radar behavior (e.g. [5], [6]), which appears as an increase in the noise floor in the estimation.

This work presents a generic description of the state-of-the-art OFDM and OTFS radar receivers under both the time-frequency and delay-Doppler plane perspectives. Based on this description, we compare the OTFS and OFDM waveform radar capabilities and the performance of different multicarrier radar receivers. A simple multicarrier radar model is presented in section II, followed by a brief description of the receivers considered in this work in section III and an evaluation of the radar performance for the various waveform-receiver pairs through simulations in section IV. In section V we present our conclusions.

II. Multicarrier Radar

OFDM and OTFS waveforms fall under the umbrella of multicarrier waveforms and can be described by the same model for multicarrier radar waveforms. Such generalization - without including OTFS - is presented in [7]. A baseband transmission equation describing such a signal may be written in the discrete domain as

$$s_{\mathrm{TX}}(k) = \sum_{n=0}^{N-1}\sum_{m=0}^{M-1} x_{n,m}\mathrm{rect}\left(\frac{kT}{N} - mT\right) \exp\left(j2\pi n\Delta f\left(\frac{kT}{N} - mT\right)\right) \quad (1)$$

where $k = 0, \ldots, NM-1$ is the sampling index of the critically sampled signal with N subcarriers and M subpulses. The duration of each subpulse is T, $\Delta f = 1/T$ is the intercarrier spacing, and $x_{n,m}$ corresponds to the modulation of the *m*-th subpulse in the *n*-th subcarrier. Equation (1) can be written in matrix form as

$$\mathbf{s}_{\mathrm{TX}} = \mathrm{vec}(\mathbf{F}_N^H\mathbf{X}) \quad (2)$$

where $\mathbf{F}_N^H$ is the IDFT matrix performing the IDFT transform along columns to create the time-signal from the time-frequency grid, and $\mathbf{X} \in \mathbb{C}^{N\times M}$ contains the phase modulation of each subpulse and subcarrier pair.

Before presenting the received signal, we define the following notation: for a delay τ and a Doppler shift f_d,

$$\psi = \exp\left(-j2\pi f_c \tau\right) \tag{3}$$

represents the phase shift due to the time delay of the carrier signal, while the Doppler shift is captured through

$$\gamma = \exp\left(-j2\pi \frac{T}{N} f_d\right) \tag{4}$$

by constructing the following matrices

$$\mathbf{\Gamma}_1 = \text{diag}\{\gamma^0, \gamma^1, \ldots, \gamma^{(N-1)}\} \tag{5}$$

$$\mathbf{\Gamma}_2 = \text{diag}\{\gamma^0, \gamma^N, \ldots, \gamma^{(M-1)N}\} \tag{6}$$

where $\mathbf{\Gamma}_1 \in \mathbb{C}^{N\times N}$ represents the Doppler phase shift along subcarriers - the ICI - and $\mathbf{\Gamma}_2 \in \mathbb{C}^{M\times M}$ is the Doppler phase shift across subpulses. Analogously, a matrix form of the target range-related subcarrier phase shift can be constructed through

$$a = \exp\left(-j2\pi\Delta f \tau\right) \tag{7}$$

with the matrix

$$\mathbf{A} = \text{diag}\{a^0, a^1, \ldots, a^{N-1}\} \tag{8}$$

Lastly, the multicarrier structure of the signal is captured by the IDFT matrix, now scaled by the Doppler shift. If we define

$$\beta_{\text{RX}} = \exp\left(j2\pi\Delta f \frac{T}{N}\left(1 - \frac{2v}{c}\right)\right), \tag{9}$$

then the scaled IDFT matrix is

$$\mathbf{B}_{\text{RX}} = \begin{bmatrix} 1 & 1 & \cdots & 1 \\ 1 & \beta_{\text{RX}} & \cdots & \beta_{\text{RX}}^{(N-1)} \\ \vdots & \vdots & \ddots & \vdots \\ 1 & \beta_{\text{RX}}^{(N-1)} & \cdots & \beta_{\text{RX}}^{(N-1)(N-1)} \end{bmatrix} \tag{10}$$

and the baseband received multicarrier signal can be written compactly as

$$\mathbf{s}_{\text{RX}} = \text{vec}(\mu\psi\mathbf{\Gamma_1}\mathbf{B}_{\text{RX}}\mathbf{A}\mathbf{X}\mathbf{\Gamma_2}) \tag{11}$$

where $\mathbf{s}_{\text{RX}} \in \mathbb{C}^{MN\times 1}$. The terms $\mathbf{\Gamma_1}$, $\mathbf{\Gamma_2}$, $\mathbf{B}_{\text{RX}}$, $\mathbf{A}$, ψ and the complex amplitude μ contain the target information. This model can be used as a common representation for different time-frequency signals, including OFDM and OTFS signals. In OFDM the communication symbols in the time-frequency plane are the entries $x_{n,m}$ of $\mathbf{X}$, whereas in OTFS the symbols are defined in the delay-Doppler domain through the matrix $\mathbf{X}_{\text{DD}}$ and transformed to the time-frequency domain via the inverse symplectic finite Fourier transform (ISFFT) (i.e. a DFT over the columns and a IDFT over the rows of X_{DD}),

$$\mathbf{X}_{\text{OTFS}} = \mathbf{F}_N \mathbf{X}_{\text{DD}} \mathbf{F}_M^H \tag{12}$$

where, by letting $\mathbf{X} = \mathbf{X}_{\text{OTFS}}$ in (2) and (11), the model can be applied for OTFS modulation. For simplicity, we assume that the cyclic prefix is long enough that no significant ISI is present in the signal.

III. Multicarrier Radar Receivers

In this section, we will introduce three different multicarrier radar receivers available in different forms in the literature.

A. Time-domain correlation

A straightforward receiver for multicarrier radar, presented in [8] and used, e.g. in [7], [9], consists of the correlation of the known time-domain signal (1) with the expected received signal (11) for all the relevant delay-Doppler pairs. Such a receiver is valid for any waveform. While it can suffer from some artifacts due to particular multicarrier frame structures such as cyclic prefixes, its main shortcoming is the high computational complexity due to the high amount of correlations to compute.

B. Symbol-canceling receiver

An alternative to such a general receiver is to design a receiver for each particular multicarrier communications waveform, using its specific frame structure. The "symbol-canceling" radar receiver [10] for cyclic-prefix OFDM (CP-OFDM) accomplishes that by reducing the complexity of the receiver to a 2D DFT, although only under the assumption of no ICI or ISI (valid for $f_d \leq 0.1\Delta f$ and τ lower than the CP duration). This is accomplished by performing an element-wise division of the received signal in the time-frequency domain $\mathbf{Y}^{\text{RX}}$ by the time-frequency communication symbols $\mathbf{X}$, that is

$$\mathbf{Y}_{n,m}^{\text{div}} = \frac{\mathbf{Y}_{n,m}^{\text{RX}}}{\mathbf{X}_{n,m}}, \tag{13}$$

and then performing a IDFT over the columns and a DFT over the rows. This is the symplectic finite Fourier transform (SFFT), i.e. the inverse transformation used to generate the OTFS time-frequency signal in (12). This receiver normalizes the received signal in the time-frequency domain, and transforms the result to the delay-Doppler domain. If $[\tau, f_d] = [0, 0]$, $\mathbf{Y}_{\text{div}}$ is an all-ones matrix, and its delay-Doppler representation $\mathbf{Y}_{\text{div}}^{\text{DD}}$ appears as a peak in $[0, 0]$. For any other pair of $[\tau_p, \upsilon_p]$, the peak in $\mathbf{Y}_{\text{div}}^{\text{DD}}$ is displaced to the corresponding index in the delay-Doppler plane. This receiver is also applicable to a OTFS signal by performing the entry-wise division in the time-frequency representation of the OTFS frame.

C. Delay-Doppler domain receiver

Lastly, a receiver can be formulated in the delay-Doppler domain, in which the OTFS symbols are defined. Such a receiver was proposed first for OTFS [4], however the formulation is valid for any multicarrier signal. Phase shifts in the time-frequency domain correspond to a translation of the signal in the delay-Doppler domain. With $\mathbf{x}_{\text{DD}} = \text{vec}(\mathbf{X}_{\text{DD}})$, and $\mathbf{y}_{\text{DD}} = \text{vec}(\mathbf{Y}_{\text{DD}})$, then

$$\mathbf{y}_{\text{DD}} = \tilde{\mathbf{H}}\mathbf{x}_{\text{DD}} + \mathbf{w} \tag{14}$$

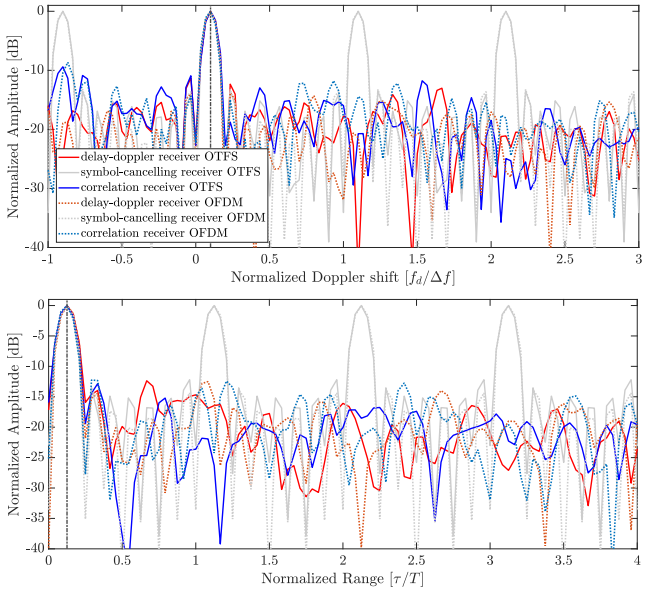

Fig. 1. Receiver output of all the presented waveform-receiver pairs for low time and Doppler shifts. Low ICI does not visibly degrade the symbol-canceling receiver. $N = 8$ and $M = 10$.

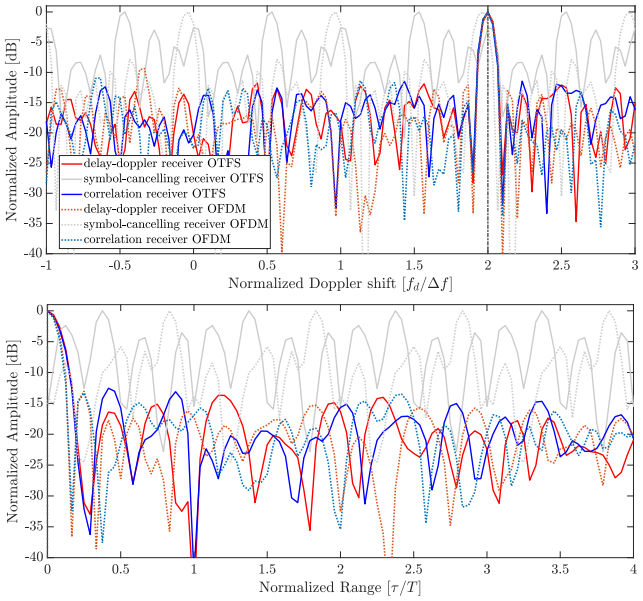

Fig. 2. Receiver output of all the presented waveform-receiver pairs for a big Doppler shift, causing strong ICI. ICI visibly degrades symbol-canceling receiver performance. $N = 8$ and $M = 10$.

where $\tilde{\mathbf{H}} \in \mathbb{C}^{NM \times NM}$. If we define a matrix $\mathbf{H}$ where the first column is equal to $\mathbf{x}_{\text{DD}}$, and the remaining columns are progressively bigger circulant shifts of $\mathbf{x}_{\text{DD}}$, then

$$\tilde{\mathbf{H}} = \mathbf{\Gamma}_1 \mathbf{H} \tag{15}$$

where $\mathbf{\Gamma}_1$ has been defined previously in (5) as a model for the ICI. Finally, the output of the receiver is given by

$$\hat{\mathbf{h}}_{\text{DD}} = \tilde{\mathbf{H}}^H \mathbf{y} \tag{16}$$

where $\hat{\mathbf{h}}_{\text{DD}} \in \mathbb{C}^{NM \times NM}$ is the receiver output for each delay-Doppler pair. A more detailed explanation on the derivation of $\tilde{\mathbf{H}}$ can be found in [4].

IV. Simulations Results

In this section, we show the simulations of the presented radar receivers for both OFDM and OTFS signals to investigate the relation between receiver and waveform performance. For this purpose, we simulate i) a scenario with $f_d \leq 0.1\Delta f$, in which the effect of ICI is tolerable for all receivers, and ii) a scenario with $f_d > \Delta f$, where the effect of ICI is very strong, and compensation or joint range-Doppler estimation is necessary. Lastly, we evaluate the integrated side lobe ratio (ISLR) (see e.g. [11] for the definition) to further understand the differences between waveforms and receivers.

A. Low-ICI scenario

We start by considering a scenario in which the Doppler shift is small enough that ICI is not a substantial issue (i.e. $f_d = 0.1\Delta f$). Fig. 1 shows the delay and Doppler receiver outputs in such a scenario. Under these conditions, it can be seen that all receivers peak at the correct range and Doppler hypotheses for both OFDM and OTFS waveforms.

Reduction of the unambiguous range and Doppler in the symbol-canceling receiver can also be noticed, with the grating lobes appearing on delays $\tau' = (nT + \tau)$ and Doppler shifts $f'_d = (m\Delta f + f_d)$. On the other hand, the Delay-Doppler and time-domain correlation receivers are capable of unambiguous estimation up to $N\Delta f$ and MT for Doppler shifts and delay, respectively. Moreover, the mainlobe does not significantly differ between receivers or waveforms. At low Doppler, the symbol canceling receiver output resembles a *sinc* function, enabling sidelobe reduction through windowing at the cost of increasing the mainlobe width. The benefits of windowing will decrease as the Doppler increases.

B. High-ICI scenario

Here we consider a high ICI scenario in which $f_d = 2\Delta f$, and compute the output of the presented receivers for both OTFS and OFDM signals. The output (see Fig. 2) shows little difference between the OTFS and OFDM in each receiver type.

The symbol-canceling receiver cannot resolve the target unambiguously in either delay or Doppler domain. This is expected, as not only is the target beyond the unambiguous hypotheses in terms of Doppler, but also the implicit assumption of no ICI in the receiver is strongly violated. Both the time-domain correlation and delay-Doppler domain receivers output reflect the correct target parameters, showing that they are not affected by ICI and that their unambiguous range and Doppler extend to the bandwidth and duration of the signal.

C. Integrated side-lobe ratio

Lastly, we evaluate the side-lobe characteristics of the presented receiver-waveform combinations for the delay

and Doppler estimation. As the main-lobe characteristics are identical for all receivers (in low ICI cases for the symbol-canceling receiver), we choose the ISLR as a metric to compare each waveform-receiver combination. We evaluate the metric within the $\tau' = [0, T]$ and $f'_d = [0, \Delta f]$ as the symbol-canceling receiver output is unusable beyond that Doppler shift. The side-lobe characteristics of the delay-Doppler and time-domain correlation receivers do not vary much for higher values of τ and f_d.

The results (see Fig. 3 and Fig. 4) show differences in the ISLR both between receivers and waveforms. Most notably, the degradation of the ISLR for the symbol-canceling receiver increases as the Doppler shifts approach Δf, and the unaccounted effect of the ICI degrades the output of the receiver. Overall, the delay-Doppler and correlation receivers show similar performance (with a notable exception for OTFS in the range estimation), and OFDM shows a lower ISLR level in Doppler estimation. In contrast, OTFS shows a lower ISLR in range estimation with the time-correlation receiver.

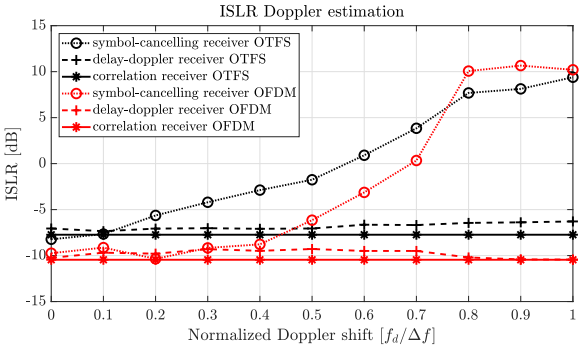

Fig. 3. Integrated side-lobe ratio in the Doppler estimation for $f_d \leq \Delta f$. $N = 8$ and $M = 10$.

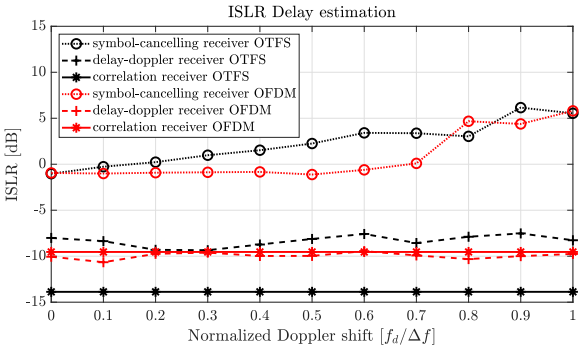

Fig. 4. Integrated side-lobe ratio in the delay estimation for $f_d \leq \Delta f$. $N = 8$ and $M = 10$.

V. Conclusions and Future Work

We presented a generic description of radar receivers associated with OTFS and OFDM multicarrier waveforms to conduct a fair comparison of the performance of OTFS and OFDM waveforms-receiver pairings. The results presented show that, for radar operation, OTFS is not more Doppler tolerant than OFDM when paired with the same symbol-canceling receiver. A joint delay-Doppler receiver, usually associated with OTFS, can achieve Doppler tolerance at the cost of higher computational complexity. Still, the same is true when this receiver is adapted to OFDM. Therefore, we conclude that receiver design can be generalized for any multicarrier waveform and that radar sensing properties usually attributed to OTFS and OFDM are, in fact, primarily due to the difference in the receivers traditionally associated with each waveform. Nonetheless, we demonstrated differences between OFDM and OTFS waveforms regarding the side-lobe characteristics for different receiver outputs.

Although the radar properties of OTFS and OFDM under the presented receivers are similar, OTFS offers the possibility of designing a signal in the delay-Doppler domain, opening exciting opportunities in terms of signal orthogonality for MIMO and new interference interactions that require further investigation.

References

[1] G. Franken, H. Nikookar, and P. V. Genderen, "Doppler Tolerance of OFDM-coded Radar Signals," in *2006 European Radar Conference*, Sep. 2006, pp. 108–111.

[2] P. Raviteja, Y. Hong, E. Viterbo, and E. Biglieri, "Practical Pulse-Shaping Waveforms for Reduced-Cyclic-Prefix OTFS," *IEEE Transactions on Vehicular Technology*, vol. 68, no. 1, pp. 957–961, Jan. 2019, number: 1 Conference Name: IEEE Transactions on Vehicular Technology.

[3] L. Gaudio, M. Kobayashi, G. Caire, and G. Colavolpe, "On the Effectiveness of OTFS for Joint Radar Parameter Estimation and Communication," *IEEE Transactions on Wireless Communications*, pp. 1–1, 2020, conference Name: IEEE Transactions on Wireless Communications.

[4] P. Raviteja, K. T. Phan, Y. Hong, and E. Viterbo, "Orthogonal Time Frequency Space (OTFS) Modulation Based Radar System," in *2019 IEEE Radar Conference (RadarConf)*, Apr. 2019, pp. 1–6, iSSN: 2375-5318.

[5] M. F. Keskin, H. Wymeersch, and V. Koivunen, "ICI-Aware Parameter Estimation for MIMO-OFDM Radar via APES Spatial Filtering," *arXiv:2102.06756 [eess]*, Feb. 2021, arXiv: 2102.06756. [Online]. Available: http://arxiv.org/abs/2102.06756

[6] G. Hakobyan and B. Yang, "A Novel Intercarrier-Interference Free Signal Processing Scheme for OFDM Radar," *IEEE Transactions on Vehicular Technology*, vol. 67, no. 6, pp. 5158–5167, Jun. 2018, conference Name: IEEE Transactions on Vehicular Technology.

[7] M. Bică and V. Koivunen, "Generalized Multicarrier Radar: Models and Performance," *IEEE Transactions on Signal Processing*, vol. 64, no. 17, pp. 4389–4402, Sep. 2016, number: 17 Conference Name: IEEE Transactions on Signal Processing.

[8] N. Levanon and E. Mozeson, "Multicarrier radar signal - pulse train and CW," *IEEE Transactions on Aerospace and Electronic Systems*, vol. 38, no. 2, pp. 707–720, Apr. 2002, number: 2 Conference Name: IEEE Transactions on Aerospace and Electronic Systems.

[9] M. Bică and V. Koivunen, "Multicarrier Radar-communications Waveform Design for RF Convergence and Coexistence," in *ICASSP 2019 - 2019 IEEE International Conference on Acoustics, Speech and Signal Processing (ICASSP)*, May 2019, pp. 7780–7784, iSSN: 2379-190X.

[10] K. M. Braun, "OFDM radar algorithms in mobile communication networks," Ph.D. dissertation, Karlsruher Institut für Technologie (KIT), Karlsruhe, 2014.

[11] M. S. Davis and A. D. Lanterman, "Minimum integrated sidelobe ratio filters for mimo radar," *IEEE Transactions on Aerospace and Electronic Systems*, vol. 51, no. 1, pp. 405–416, 2015.